Proceedings of the 7th European VLBI Network Symposium
Bachiller, R. Colomer, F., Desmurs, J.F., de Vicente, P. (eds.)
October 12th-15th 2004, Toledo, Spain

Powerful Extragalactic Hydroxyl Emitters

Hans-Rainer Klöckner[1,2] and Willem A. Baan[2]

[1] Astrophysics, Denys Wilkinson Building, Oxford University, Keble Road, Oxford, OX1 3RH, Great Britain

[2] ASTRON, Westerbork Observatory, P.O. Box 2, 7990 AA Dwingeloo, The Netherlands

Abstract. Activity in the centers of galaxies is powered by nuclear starbursts on scales of up to 1000 pc as well as by true active galactic nuclei, which are compact luminous sources that reside in the central parsecs of quasi-stellar objects (QSOs), radio galaxies, and Seyfert galaxies. Different physical aspects of the circum-nuclear medium serve as trigger for these forms of nuclear activity and it seems paradoxical that low-energy molecular processes serve as probes of the hostile, energetic environments of such nuclei.
Hydroxyl Megamaser emission is one of these low-energetic processes. This paper reviews the general emission properties and studies of individual sources at spatial resolution between tens to hundred of parsec. It will be shown that such emission does provide a critical view of the physical conditions in an active nucleus.

1. Introduction

Hydroxyl (OH) Megamaser emission was discovered in the early eighties as a new sort of extragalactic maser emission with isotropic luminosities of six or more orders of magnitudes higher than the Galactic sources. Based on the location, the extreme luminosity, and the exceptional line width, it has been speculated that this Megamaser emission would sample the circum-nuclear environment and expose the nuclear properties of the host galaxies (Baan et al., 1982).
The main characteristic of this extraordinary emission is the strong association with the enhanced infrared emission of the host galaxy. In fact, the prototype Ultra-Luminous Infrared Galaxy (ULIG) Arp 220 was known to be an OH emitter before its dramatic infrared properties were discovered. These galaxies are extreme in various ways. They show emission properties that are either dominated by their constituent stars or by a significant non-stellar emission process. They are believed to display a transient stage in galaxy formation, where, due to a galaxy merger, material is transported into the nuclear region. The large amount of material that is transported towards the nuclear region causes enhanced star-formation and could feed a super-massive black hole, the important ingredient of a nuclear engine for QSOs (Sanders et al., 1988). Such regions are difficult to access since large amounts of material block most of the visible light. However, the OH Megamaser emission in the radio regime provides a unique view to the incubator of the nuclear power.
In this paper an overview will be given of the current status of the OH Megamaser (OHMM) population and our understanding of the physical processes causing such emission. In addition, the OH emission down to parsec scales will be discussed and its contribution to the general understanding of the nuclear environment.

2. The Population

Since their discovery in the early eighties, an enormous effort has been undertaken to expand the sample of hydroxyl Megamaser galaxies (Schmelz et al., 1986; Garwood et al., 1987; Norris et al., 1989; Staveley-Smith et al., 1992; Baan et al., 1992; Darling & Giovanelli, 2000, 2001, 2002a). At present about one hundred galaxies have been quoted in the literature to exhibit OH emission. These sources were found in searches based on the infrared properties and resulted in low detection rates of a few percent. These detection rates either indicate that the OHMM emission is a rare process or that the selection criteria are inadequate and that the OHMM emission sources have additional characteristics, which have not been found so far. From the 100 sources with claimed OH emission, the OH emission spectra of 25 sources are either unpublished or are limited by their sensitivity to make a clear determination of hydroxyl main-line emission. By evaluating the individual sources, the Megamaser sample has been reduced to 74 sources with OH luminosities larger than 1 $L_\odot$, which will make up the database for evaluating the general properties (Klöckner, 2004).

2.1. How complete are we ?

The current sample of OHMM galaxies is compiled from different data sets that are based on varied selection criteria. In order to draw conclusions and to constrain the common properties of the OHMM sources, the completeness of the used sample needs to be examined. The V/V_{max}-test is a direct method to investigate the uniformity of the distribution of objects in space and may be used for this purpose (Schmidt, 1968). For a galaxy with a luminosity of $L \sim r^2 \, S \, \Delta v$ at a distance r, with a flux density S, and with a line width of Δv, the quantity V/V_{max} describes the completeness of the sample. V is the volume of space enclosed by the survey and V_{max} is the volume of space

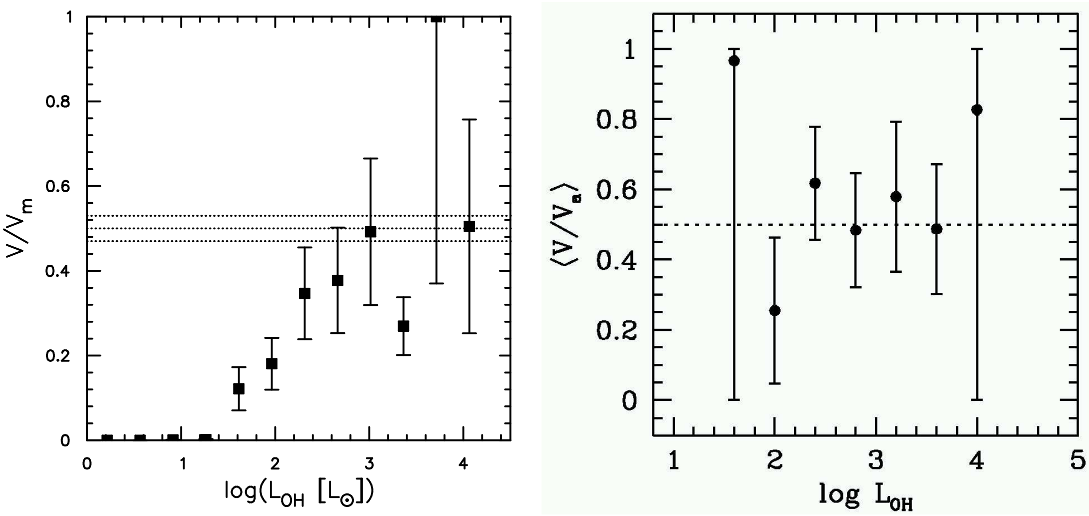

Fig. 1. The V/V_{max}-test for two different data bases. Left panel: the database used in this paper. Right panel: A limited OHMM sample with $f_{60\mu m}$ >0.6 Jy (Darling & Giovanelli, 2002b). Note that the OH luminosity range is different for the two panels and that in the right panel sources with z>0.23 are excluded.

within which this source would still be included into the sample. The value of V/V_{max} would range between 0 and 1 if the sources have constant co-moving number densities. For studies of extragalactic objects, the statistics of the complete sample are often limited; therefore this test is used to evaluate the completeness of the new (reduced) OHMM sample.

The estimates of the V/V_{max}-test for the sample of 74 sources are displayed in the left panel of Figure 1. For comparison the right panel shows these estimates for a OHMM sample based on more uniform selection criteria. This reference sample is an OHMM sample selected on an infrared flux of $f_{60\mu m}$ >0.6 Jy, accessible with Arecibo, and a redshift between 0.1 to 0.45 (Darling & Giovanelli, 2002b); systematic effects cannot be ruled out for this dataset. The diagrams show clear differences in their distribution; for the uniformly distributed sample a value of about 0.5 would be expected. The new OHMM database shows systematically lower V/V_{max} values in comparison with the other sample. Especially at lower luminosities this database diverges from an uniform distribution. In should be noted that the observed incompleteness at lower luminosities may also be caused by sources with extreme redshifts because the volume boundary V_{max} is determined by the maximum redshift present in the sample. Since these sources may have almost Giga-maser luminosities, they could cause an undersampling of the tested volumes at lower luminosities. The test indicates a range at intermediate luminosity where the sample galaxies deviate from a uniform distribution; this effect may be related to the enhanced maximum volume or another unknown reason. Excluding sources at larger redshift the new database will help the distribution, but some of the under-sampling will remain. Similar effects can be expected from the reference sample if the high redshifted sources are included.

Both samples show evidence that OHMM galaxies are undersampled in some luminosity ranges. Therefore, in evaluating the geneal properties of the OHMM sample at other wave bands, the incompleteness in these luminosity ranges needs to be taken into account.

2.2. The galactic morphology

In the optical, the OHMM are found to be morphologically peculiar sources, that are generally associated with interacting galaxies (Staveley-Smith et al., 1989). The Digitized Sky Survey has been used to investigate the morphological structure of 65 of the 74 sampled sources. For these 65 sources: 2 are spiral galaxies, 6 are elliptical galaxies, 26 show multiple sources or interactions as traced by tails or distorted isophotes, and 31 are unresolved point sources at a pixel resolution of about $1-2''$. Hence the optical morphology of most OH Megamaser galaxies remains inconclusive.

2.3. The infrared properties

The most outstanding attribute of OHMM galaxies is their exceptional infrared luminosity that covers almost three orders of magnitude ranging between 2×10^{10} $L_\odot$ and 1×10^{13} $L_\odot$. Based on the classification of galaxies displaying infrared excess, the OHMM sources are part of the sample of Luminous Infrared Galaxies and Ultra Luminous Infrared Galaxies (the different criteria for LIG and ULIG are listed in Table 1 of Sanders & Mirabel, 1996). Five sources in our sample show infrared luminosities of less than 10^{12} $L_\odot$ (LIG), whereas the other sources are a sub-sample of the ULIG population. It is interesting to note that at infrared luminosities of about 10^{12} $L_\odot$ all objects show evidence for a merger activity (Sanders 2004, private communication) and therefore the OHMM galaxies are directly linked to the formation of an active nucleus.

A detailed review of the infrared properties of 18 emitters and 24 absorbers showed that galaxies with OH in absorption have colder infrared spectra than OH emitters (Baan, 1989). Here

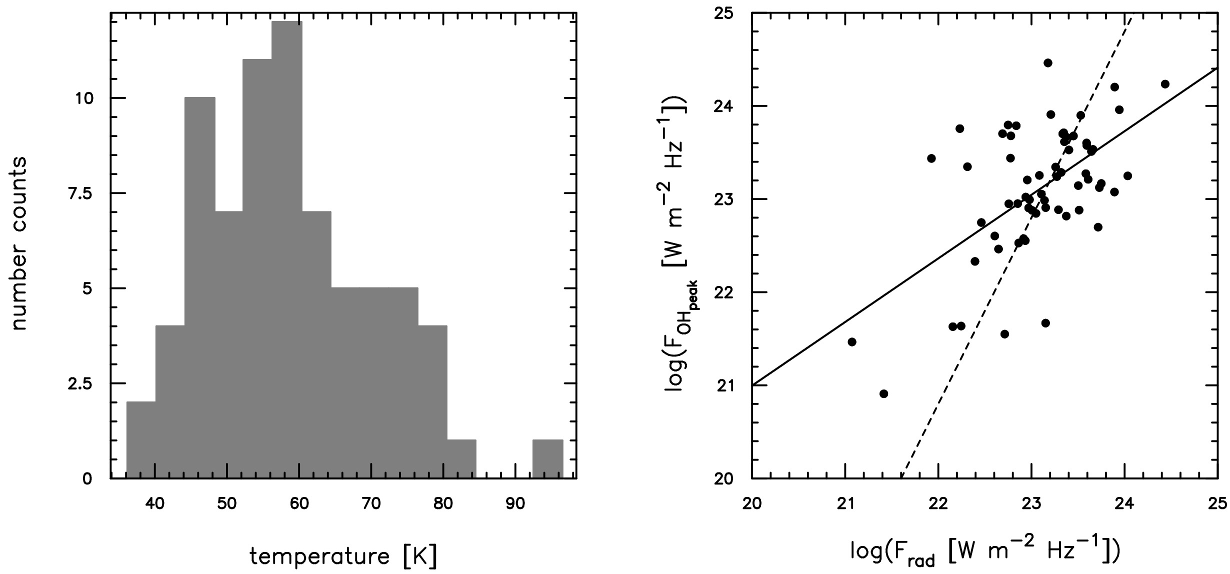

Fig. 2. Left panel: Histogram of the infrared temperature of the sources in the OH Megamaser sample estimated from the IRAS database (Klöckner, 2004). Right panel: The OH flux density versus the radio continuum flux density. The solid line displays the estimated linear relation between these quantities. The dashed line indicates a slope of 2.

we consider a similar investigation for OH emitters only. For this purpose, the infrared luminosity is estimated by a χ^2-fit of a single black body to the fluxes in the 4 IRAS bands at 12, 25, 60, and 100 μm (data compiled from the IRAS Faint Source Catalog; Moshir et al., 1992). The temperature estimates of the sample are displayed in the histogram in the left panel of Figure 2. The histogram indicates a maximum temperature of about 97 K and a broad distribution of temperatures ranging from 50 K to 80 K. The distribution of the infrared temperature peaks at around 59 K. This value is consistent with theoretical investigations that show that OH main-line emission is produced by a diluted black body emission spectra peaking around 60 K (Klöckner & Baan, 2004b; Randell et al., 1995). This confirms that the intense far-infrared radiation field serves as a radiative pump for producing an inverted population of OH molecules (Baan, 1985; Klöckner, 2004).

This clear association of the OH emission with the infrared emission suggests that OH is a good tracer of the dusty circumnuclear environment. Such an environment plays a central role in the unification scheme of active galaxies and turns OH Megamaser emission into a unique probe for investigating the geometry and physics of the dusty structures in active nuclei (Antonucci & Miller, 1985).

2.4. The integrated hydroxyl emission

The correlation of the OH emission with the infrared emission indicates that the intense far-infrared radiation provides the energy source responsible for the excitation of the OH molecules, and therefore of the maser emission (Baan, 1985). The conversion factor of the integrated infrared photons into OH maser photons has been found to be less than a percent (Klöckner, 2004). Such conversion factors suggest that the integrated OH Megamaser emission is caused by an unsaturated maser process (Elitzur, 1992). Nevertheless, saturation effects cannot be generally ruled out and have been claimed to be present in filaments of parsec scales in three bright OH emitters Arp 220, III Zw 35, and IRAS 17208−0014 (Lonsdale et al., 1998; Diamond et al., 1999). The determination of the amplification factors and the measure of saturation requires a crucial assumption that may not hold for these high-resolution observations of the OH emission. The saturated maser emission from these filaments provides only a minor contribution to the overall OH emission and can be neglected.

In order to estimate the hydroxyl abundance responsible for the OHMM emission, it can be assumed that the OH emission results from amplification of a background radio continuum emission. Under this assumption the integrated properties of the radio and the OH emission should be correlated. The distribution in Figure 2 shows this relation and can be described with a slope of (0.68±0.12) and an intercept point of $\log(\mathrm{F_{OH}})$ at (7.13±2.8). For an unsaturated maser (I) the radiative transfer equation may be written as:

$$\mathrm{I} = \mathrm{I_0}\, \mathrm{e}^{\kappa \mathrm{l}} + \frac{\epsilon}{\kappa}\left(\mathrm{e}^{\kappa \mathrm{l}} - 1\right), \qquad (1)$$

where $\mathrm{I_0}$ is the external continuum emission, $\kappa\, l$ is the unsaturated gain, ϵ is the self emission of the gas, and l is the path length. In the case that self emission is negligible, this equation can be compared with the linear relation of Figure 2. Applying this correlation to the following equations, the OH column density can be determined (Reid & Moran, 1981):

$$\kappa \mathrm{l} = \frac{\mathrm{h}\nu_0 \mathrm{B}}{4\pi\Delta\nu} \frac{\Delta \mathrm{n}}{1 + \frac{2\mathrm{C}}{\mathrm{P}}} \qquad (2)$$

where B is the Einstein coefficient, $\Delta\nu$ is the Doppler width of the line, Δn is the population inversion and the factor $(1 + \frac{2\mathrm{C}}{\mathrm{P}})$ accounts for the effects of collisional (C) and radiative (P)

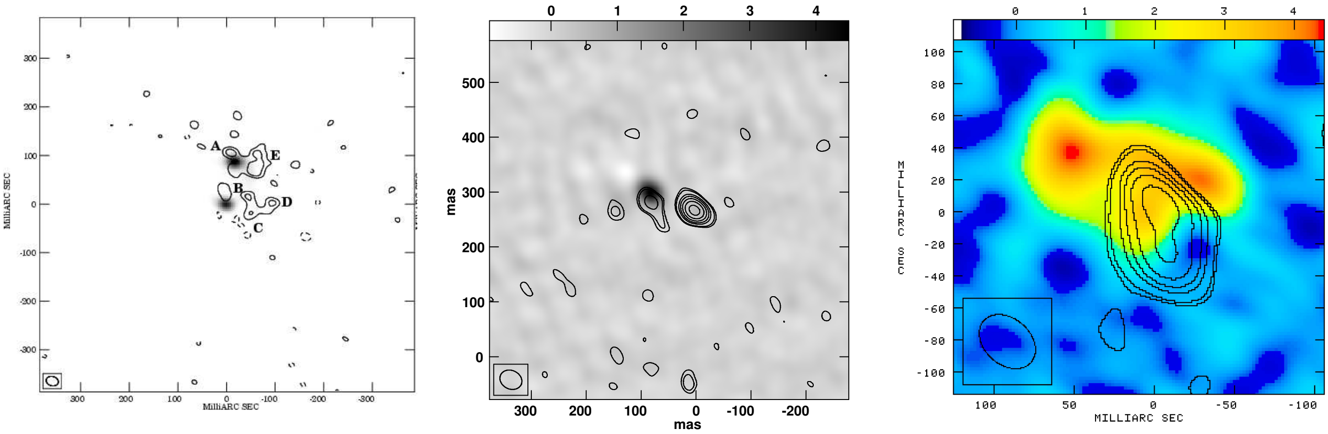

Fig. 3. OH Megamaser sources seen with the EVN. The 1667 MHz maser line in gray scale with the radio continuum emission in contours superimposed. Left panel: III Zw 35 seen with spatial resolution of 25×19 mas; middle panel: Mrk 273 with 41×34 mas; right panel: Mrk 231 with 39×28 mas.

pumping rates. This ratio may be determined by the ratio of the 1720 MHz and the 1667 MHz emission, where theoretical modelling indicates that collisional effects are responsible for the 1720 MHz line emission (Wardle, 1999). For a few OH Megamaser sources these emission lines have been detected, which give ratios on the order of 0.07 or less (Baan et al., 1989). With an average line width of about 171 km s^{-1} determined from the sample galaxies, a column density of approximately 6.4×10^{13} cm^{-2} needs to be inverted to amplify an averaged radio luminosity of $\sim 1^{23}$ W m^{-2} Hz^{-1}. The relation indicated by the dashed line in Figure 2 would result in a column density of 1.5×10^{17} cm^{-2}. OH in absorption with a similar line structure and an excitation temperature of 44 K (Henkel et al., 1986) would give a column density of about 6.4×10^{16} cm^{-2}. Comparing the findings of the two relation between the F_{OH} and F_{rad} with OH in LTE we find for the solid line in Figure 2 that one molecule out of 1000 molecules be required for amplification and for the dashed line some 700 out of 1000 are required.

A question that remains unanswered if 99.9 % of the OH is not inverted than self-absorption may play a crucial role. On the other hand if self emission does not play a role than the OH would mimic the continuum emission structure. But this is not an indication of saturated maser action. Further modelling of the individual OH transitions is needed to provide better estimates of the molecular content within OHMM galaxies.

3. Hydroxyl at Small Angular Resolution

With the first high-resolution observations of OH Megamaser sources it has become clear that some of the line and continuum emission characteristics can be studied in great detail within the nuclear region of active galaxies. A list of OHMM sources observed with very-long-baseline-interferometry is shown in Table 1. A complicating factor in such investigations is that the OH maser emission shows components with varying degrees of compactness at a resolution of a few parsecs. In addition, some of these observations resolve almost ~90 % of the total continuum and some ~50 % of the OH flux measured with a single-dish or a low resolution interferometer array. Generally the strongest remaining line emission feature is the 1667 MHz line, while the 1665 MHz line tends to be mostly resolved at such resolution. Such effect indicate that the pumping conditions change at different scale sizes, which complicates the interpretation of the OH Megamaser emission. Examples of this effect are found in Arp 220, IRAS 17208−0014 and IRAS 10039−3338 observed with global VLBI (Lonsdale et al., 1998; Diamond et al., 1999; Rovilos et al., 2002) or in the nearby source IC 694 observed with the EVN (Klöckner & Baan, 2002). This makes it difficult to interpret and understand the unusual OH emission components, but it also suggests that the OH emission provides unique information about the colder phase of the ISM at scales between a few tens of parsecs and hundreds of parsecs.

If such difficulties prevent finding the secrets of these sources, why do we bother? OHMM sources with warm infrared colors may provide a possible evolutionary connection between ULIGs and QSOs, where the ULIGs are part of a sequence of merging spiral galaxies (Klöckner, 2004; Sanders & Mirabel, 1996). After funnelling gas into the merger nucleus, which feeds a nuclear starburst, a self-gravitating gas disk on scales of about 1 kpc may be formed (Taylor et al., 1999; Sanders & Mirabel, 1996). Such a scenario is possibly found in OH Megamaser sources, where the presence of a starburst and/or a disk/torus structure has been reported in the circum-nuclear region at a spatial resolution of tens of parsec (Lonsdale et al., 1998; Pihlström et al., 2001; Klöckner & Baan, 2004a).

Prime examples for nuclear starbursts are the two nuclei of the classical OH Megamaser Arp 220. In the radio continuum emission the ongoing burst of star formation is traced by radio supernovae (Lonsdale 2004 preliminary results, Smith et al., 1998). The OH emission at larger scale sizes (~175 pc, ~280 pc) at both regions of starburst activity provides clear evidence of structured kinematics that can be associated with nuclear disks. The OH emission at parsec scales shows a rather poor association with the continuum emission, as would be expected for the classical OH Megamaser model (Baan, 1989). However, such a lack of association can be caused by the spatial response of the array, because the more diffuse continuum emission is resolved and the higher brightness OH emission produced by the superposition of individual emitting region/clouds remains visible. In general, the hydroxyl emission at Arp 220 shows numerous line features at parsec scales, in emission as well as in absorption, and at various velocities. These need to be studied in greater detail to provide the molecular abundances of these regions.

The existence of a disk or torus has been concluded from detailed and sensitive studies of the OH Megamasers III Zw 35, Mrk 273, and Mrk 231 (Pihlström et al., 2001; Klöckner & Baan, 2004a; Klöckner et al., 2003). Figure 3 shows the continuum emission and the integrated OH line emission in these sources, which provides first clues of the nuclear nature. In particular, for III Zw 35 the radio emission structure seems to be resolved, whereas for the other objects discrete point sources remain. The overall infrared temperature of this sources increases (from left to right 64 K, 68 K, 79 K). The ratio between the infrared and the radio emissions would indicate a higher probability for an accretion related circum-nuclear engine in Mrk 231. Evidence of nuclear accretion in Mrk 231 is also provided by other wavelength studies, that show Seyfert 1 line characteristics and an energetic radio outflow from the nucleus (Baan et al., 1998; Ulvestad et al., 1999a). However, its seems that the total radio power of this source is not accretion dominated after all and therefore a combination of a nuclear starburst and an AGN seems most likely in Mrk 231 and Mrk 273 (Taylor et al., 1999; Carilli & Taylor, 2000). One way to trace such embedded engines is to use the kinematic information from the maser emission within the nuclear starburst region. In the case of III Zw 35, a starburst disk has been reported with an outer size of about 86 pc and an enclosed mass of 7×10^{6} $M_{\odot}$ (Pihlström et al., 2001). The galaxy Mrk 273 shows a diffuse continuum structure indicating a starburst nucleus that is punctuated by compact sources (Carilli & Taylor, 2000). Within that structure the OH emission traces the dynamics of an edge-on thick disk or torus of 108 pc, that is oriented almost perpendicular to the kinematic structure at larger scales. The velocity structure suggests an AGN with a central binding mass of 1.4×10^{9} $M_{\odot}$ (Klöckner & Baan, 2004a). Similarly the source Mrk 231 shows OH emission embedded in a starburst disk (Taylor et al., 1999). Compared with other sources in the OH Megamaser sample, the location of the nuclear engine is known to parsec scales and its radio outflow extends to almost hundred parsec (Ulvestad et al., 1999a,b). The OH emission extends for one hundred pc and displays a half-circular shape straddling the nuclear radio outflow. Modelling of the emission structure suggests an inclined thick disk or torus of 200 pc in size with an enclosed mass of 7.2×10^{9} $M_{\odot}$ (Klöckner et al., 2003).

More sources have been observed with VLBI techniques but they do not reveal clear evidence of a circum-nuclear structures. The reason is most likely the inadequate spatial sensitivity of the VLBA/EVN data sets.

Table 1. OH Megamaser galaxies observed at milli arcsecond (mas) resolution.

source	dist [Mpc]	1 mas [pc]	instrument
IC 694(Arp 229)	42	0.20	EVN[g], MERLIN[j]
Arp 220	73	0.35	VLBI[b]
III Zw 35	111	0.54	VLBI[c], VLBA[d], EVN[e]
IRAS 10039 − 3338	137	0.67	VLBA[l]
Mrk 273	154	0.74	EVN[q], MERLIN[h,i]
Mrk 231	172	0.83	EVN[f], MERLIN[h]
IRAS 17208 − 0014	175	0.82	VLBI[c]
IRAS 10173 + 0828	194	0.94	EVN[o]
IRAS 08201 + 2801	698	3.38	EVN[p]
IRAS 10339 + 1548	822	3.98	EVN[p]
IRAS 12032 + 1707	910	4.41	VLBA[k], EVN[p]
IRAS 14070 + 2505	1118	5.42	VLBA[k]

The distance is determined by assuming q_0 = 0.5 km s^{-1} and H_0 = 75 km s^{-1} Mpc^{-1}.

References: b – Lonsdale et al. 1998, c – Diamond et al. 1999, d – Trotter et al. 1997, e – Pihlström et al. 2001, f – Klöckner et al. 2003, g – Klöckner & Baan 2002, h – Richards et al. 2000, i – Yates et al. 2000, j – Polatidis & Aalto 2000, k – Pihlström et al. 2004 in prep., l – Rovilos et al. 2002, o – Klöckner et al. 2004 in prep., p – Rovilos 2004, q – Klöckner & Baan 2004a.

– The source IRAS 10039−3338 has been observed with the VLBA and the phased VLA for 33 minutes only. Around 67 % of the total 1667 MHz line emission has been detected, but no continuum or 1665 MHz line could be found (Rovilos, 2004). The dominant spectral signature of the single-dish spectrum shows three individual line features, which have been recovered by these observations (Killeen et al., 1996). This spectral signature is similar to that of the OH emission seen in Mrk 273, where evidence of a rotating disk has been reported. For IRAS 10039−3338 more observations are needed to be able to make such conclusions.
– The continuum and OH line emission in the source IRAS 17208−0014 display the general observational characteristics of OH Megamaser sources. The source was observed with global experiment using EVN and VLBA, where the USA telescopes participated for 3 hrs, resulting in a spatial resolution of 8×58mas. The OH emission recovered in the data is about 20 % of the single-dish flux and it is confined in a single/or double line feature of 200 km s^{-1} in width (Diamond et al., 1999).
– IRAS 08201+2801 has been observed with the EVN. The OH emission has only been detected in WSRT-EB-JB triangle (62 mas). The spectral signature of the emission line features detected on the individual baselines shows a possible double peak structure with a separation of about 132 km s^{-1}. Such a spectral signature could represent the kinematics of a starburst disk like in III Zw 35. The continuum has been detected with 3 or 5.9 mJy (Rovilos, 2004) and combined with the line peak flux density no or moderate amplification can be deduced.
– The OH emission of the source IRAS 10339+1589 have been marginally detected in the baselines between Effelsberg and Westerbork of the EVN array (Rovilos, 2004). Upper limits are given for the continuum and the OH emission of 3.9 and 6.9 mJy/beam respectively. In comparison with the Single-dish measurements, these observations recover all of the OH emission. For the upper limits a moderate amplification of 0.57 can be estimated.

- The source IRAS 12032+1707 has been observed by the EVN (Rovilos, 2004) and by the VLBA (Pihlström et al. 2004 in prep.). The EVN observation give upper limits of 0.69 and 2.1 for the continuum and line emission respectively. Whereas the VLBA observation recovers the total line flux density detected with the single-dish.
- For IRAS 14070+0525 only a small fraction of the OH emission has been recovered by the VLBA (Pihlström et al. 2004 in prep.). Such emission is confined to a region of about 20×20 mas. The peak line flux density is about 2.25 mJy and no continuum could be recovered.

4. Conclusions

Much effort has been invested in observing and understanding the OH Megamaser phenomenon. Only recently these efforts have begun to pay off and extragalactic OH emission has shown us some of its beauty. However, there is still need for further investigation of the theoretical frameworks as well as in the observational domain. Little is known about the diffuse OH emission. The detection of this emission could open a new field of research for studying the molecular gas phase all the way from the galactic environment at several kilo parsecs to the nuclear regions of active galaxies. In particular, the EVN network with its new telescopes is the prime instrument for study of such OH Megamaser emission at various scale sizes.

Acknowledgements. The European VLBI Network is a joint facility of European, Chinese, South African and other radio astronomy institutes funded by their national research councils. This research was supported by the European Commission's I3 Programme "RADIONET", under contract No. 505818.

References

Antonucci R.R.J., Miller J.S.: 1985, *ApJ*, 297, 621
Baan W.A.: 1985, *Nature*, 315, 26
Baan W.A.: 1989, *ApJ*, 338, 804
Baan W.A., Haschick A., Henkel C.: 1992, *AJ*, 103, 728
Baan W.A., Haschick A.D., Henkel C.: 1989, *ApJ*, 346, 680
Baan W.A., Salzer J.J., Lewinter R.D.: 1998, *ApJ*, 509, 633
Baan W.A., Wood P.A.D., Haschick A.D.: 1982, *ApJ Lett.*, 260, L49
Carilli C.L., Taylor G.B.: 2000, *ApJ Lett.*, 532, L95
Darling J., Giovanelli R.: 2000, *AJ*, 119, 3003
Darling J., Giovanelli R.: 2001, *AJ*, 121, 1278
Darling J., Giovanelli R.: 2002a, *AJ*, 124, 100
Darling J., Giovanelli R.: 2002b, *ApJ*, 572, 810
Diamond P.J., Lonsdale C.J., Lonsdale C.J., Smith H.E.: 1999, *ApJ*, 511, 178
Elitzur M.: 1992, Astronomical masers. Astronomical masers Kluwer Academic Publishers (Astrophysics and Space Science Library. Vol. 170), 365 p.
Garwood R.W., Dickey J.M., Helou G.: 1987, *ApJ*, 322, 88
Henkel C., Guesten R., Batrla W.: 1986, *A&A*, 168, L13
Killeen N.E.B., Staveley-Smith L., Wilson W.E., Sault R.J.: 1996, *MNRAS*, 280, 1143
Klöckner H.R.: 2004, *Ph.D. Thesis; Rijksuniversiteit Groningen*
Klöckner H.R., Baan W.A.: 2002, In: *IAU Symposium 206: Cosmic Masers: from protostars to blackholes; 2001, Mangaratiba, Rio De Janeiro, Brazil; eds. V. Migenes, M.J. Reid;Astronomical Society of the Pacific, San Francisco*, pp. 430–433
Klöckner H.R., Baan W.A.: 2004a, *A&A*, 419, 887
Klöckner H.R., Baan W.A.: 2004b, In: *the 2004 European Workshop: "Dense Molecular Gas around Protostars and in Galactic Nuclei", Eds. Y.Hagiwara, W.A.Baan, H.J.van Langevelde, 2004, a special issue of ApSS, Kluwer*
Klöckner H.R., Baan W.A., Garrett G.A.: 2003, *Nature*, 421, 821
Lonsdale C.J., Lonsdale C.J., Diamond P.J., Smith H.E.: 1998, *ApJ Lett.*, 493, L13
Moshir M., Kopman G., Conrow T.A.O.: 1992, IRAS Faint Source Survey, Explanatory supplement version 2. Pasadena: Infrared Processing and Analysis Center, California Institute of Technology, 1992, edited by Moshir, M.; Kopman, G.; Conrow, T. a.o.
Norris R.P., Gardner F.F., Whiteoak J.B., Allen D.A., Roche P.F.: 1989, *MNRAS*, 237, 673
Pihlström Y.M., Conway J.E., Booth R.S., Diamond P.J., Polatidis A.G.: 2001, *A&A*, 377, 413
Pihlström Y.M., Baan W.A., Darling J., Klöckner H.-R.: 2004, *ApJ*, in prep.
Polatidis A.G., Aalto S.: 2000, In: *5th EVN Symposium 2000, Eds.: J.E. Conway, A.G. Polatidis, R.S. Booth and Y.M. Pihlström, published Onsala Space Observatory, p. 127*
Randell J., Field D., Jones K.N., Yates J.A., Gray M.D.: 1995, *A&A*, 300, 659
Reid M.J., Moran J.M.: 1981, *ARA&A*, 19, 231
Richards A., Cohen, Cole, et al.: 2000, In: *IAU Symposium*, vol. 205
Rovilos E.: 2004, *Ph.D. Thesis; University of Manchester*
Rovilos E., Diamond P.J., Lonsdale C.J., Smith H.E.: 2002, In: *New Developments in VLBI Science and Technology*, pp. 179–+
Sanders D.B., Mirabel I.F.: 1996, *ARA&A*, 34, 749
Sanders D.B., Soifer B.T., Elias J.H., et al.: 1988, *ApJ*, 325, 74
Schmelz J.T., Baan W.A., Haschick A.D., Eder J.: 1986, *AJ*, 92, 1291
Schmidt M.: 1968, *ApJ*, 151, 393
Smith H.E., Lonsdale C.J., Lonsdale C.J., Diamond P.J.: 1998, *ApJ Lett.*, 493, L17+
Staveley-Smith L., Allen D.A., Chapman J.M., Norris R.P., Whiteoak J.B.: 1989, *Nature*, 337, 625
Staveley-Smith L., Norris R.P., Chapman J.M., et al.: 1992, *MNRAS*, 258, 725
Taylor G.B., Silver C.S., Ulvestad J.S., Carilli C.L.: 1999, *ApJ*, 519, 185
Trotter A.S., Moran J.M., Greenhill L.J., Zheng X., Gwinn C.R.: 1997, *ApJ Lett.*, 485, L79
Ulvestad J.S., Wrobel J.M., Carilli C.L.: 1999a, *ApJ*, 516, 127
Ulvestad J.S., Wrobel J.M., Roy A.L., et al.: 1999b, *ApJ Lett.*, 517, L81
Wardle M.: 1999, *ApJ Lett.*, 525, L101
Yates J.A., Richards A.M.S., Wright M.M., et al.: 2000, *MNRAS*, 317, 28